ORIGINAL ARTICLE

lajss.org© Latin American Journal of Solids and Structures

www.lajss.org

DYNAMIC ANALYSIS OF A COUPLED HIGH-SPEED TRAIN AND BRIDGE SYSTEM SUBJECTED TO SEA WAVE HYDRODYNAMIC LOAD

Amin Razzaghi Kalajahi[a], Morteza Esmaeili[a]*, Jabbar Ali Zakeri[a]

[a] School of Railway Engineering, Iran University of Science and Technology, Tehran, Iran. E-mail: amin_razzaghi@rail.iust.ac.ir, m_esmaeili@iust.ac.ir, zakeri@iust.ac.ir

•Corresponding author

https://doi.org/10.1590/1679-78256139

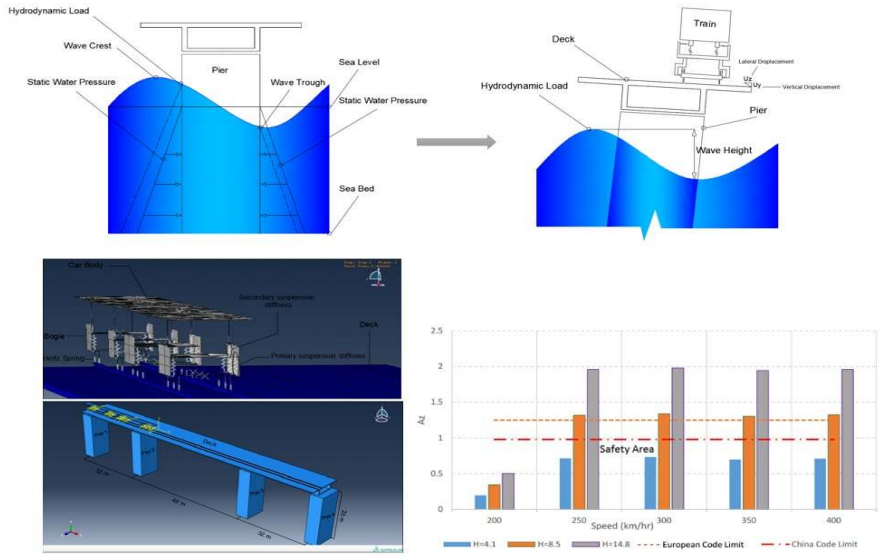
Abstract

In this study, the dynamic behavior of the 3D train–bridge system subjected to different hydrodynamic loads (TBW model) is established. By taking a continuous bridge with box girders as a case study, the dynamic responses of the bridge which is under train passing and subjected to several sea hydrodynamic loads are analyzed. Hydrodynamic forces are applied on piers according to Morison's theory and car body is modeled by a 27-DoFs dynamic system. Model validation has been performed with other research by considering vessel collision load. In continuation, the dynamic responses of the bridge and the running safety indices of the train on the bridge under several conditions are analyzed. Consequently an assessment procedure is proposed for the running safety of high-speed trains on bridges subjected to wave loads. Results of TBW's sensitive analyzes have shown the importance of sea-states conditions for train safe and comfortable running. These outputs indicates that in stormy conditions, the speed of the train crossing the bridges should be reduced and it is possible for the train to pass at low speeds in stormy conditions.

Keywords

Train-bridge-wave (TBW); hydrodynamic load; high-speed; running safety

Graphical Abstract



Received: May 31, 2020. In Revised Form: November 22, 2020. Accepted: December 22, 2020. Available online: January 08, 2021.
https://doi.org/10.1590/1679-78256139

Latin American Journal of Solids and Structures. ISSN 1679-7825. Copyright © 2021. This is an Open Access article distributed under the terms of the Creative Commons Attribution License, which permits unrestricted use, distribution, and reproduction in any medium, provided the original work is properly cited.

1 INTRODUCTION

Today, the use of rail transportation system has been accepted as one of the best transportation modes in the most developed countries. In these countries, high-speed trains play a major role in passenger transportation management and are always in the center of attention. One of the important structures in the railroad are bridges that are constructed with different length and spans over the rail routes and make the traffic of the rail vehicles possible with acceptable quality (Jahangiri and Zakeri 2017). Bridges are one of the most critical and important railway structures that may need to be built in challenging locations, one of these is the construction of bridges to cross the waterways safely. River/Sea crossing bridge is one of the common infrastructures for the extension of rail from the mainland to the islands or coastal areas (Fang et al. 2018). The behavior of bridges is affected by different loads and special attention needs to be paid to this. The loads on the railway bridges vary in terms of axle load, running speed and volume of the yearly traffic and affect the behavior of the railway bridges, so extensive studies have been carried out in this regard. Dynamic bridge-train interaction is one of the topics that has attracted the attention of railway engineers over the past thirty years. Train operational parameters are the most important factors affecting the behavior of bridges, consequently many studies have been carried out to resolve the vibration problems and ensure the vehicle–bridge coupling system's performance. In this regard, the works of (Frýba 1996; Ji et al. 2012; Kaloop et al. 2016; Hassan and Saddiq 2016; James 2003; Liu et al. 2009; Dadashzadeh and Zakeri 2013; Jahangiri and Zakeri 2017) can be pointed out. Museros et al. 2002 has investigated the use of a moving load model for short-span bridges. Other Studies on the horizontal displacements in structural frames under vertical forces are discussed (Ellis et al. 2003). On the other hand, various studies have been conducted to simulate the behavior of bridges against earthquakes and winds (Miyata and Koji 1993; Yasuda et al. 2000; W. T. Yim 2007). Further appropriate research has been done on the lateral dynamic behavior of railway bridges (Dias and Silva 2007). Other researches on how to model train-bridge interactions using two models of moving load or mass-spring model have been done (Liu et al. 2009; Hughes 2010; Rigueiro et al. 2010; Höghastighetsprojekt 2010; Bargi and Aghabozorgi 2010), and have provided suggestions on how to model the train-bridge interactions, and have presented results about ineffectiveness of modeling all components of bridges with spans greater than 15 m (Varandas et al. 2011; Rashid 2011). Other articles have been written about bridge behavior under train moving load with considering bridge's damping ratio, span length and deck materials (Bouassida et al. 2012; Dadashzadeh and Zakeri 2013; Hassan and Saddiq 2016; Kaloop et al. 2016). Train moving load on bridge is also performed by ANSYS software (Melaku and Hongsheng 2014). A 3D FEM which is employed in Abaqus finite element software to model and analyze the bridge and train while considering the interaction between them using the Hertz theory has been presented (Jahangiri and Zakeri 2017).

As is clear, bridges are indispensable structures for crossing rivers, bays and other railway or highway lines, while sometimes they also become man-made obstacles against water flow or traffic underneath. With the rapid expansion of the infrastructure network in the past decades, more crossings are generated being the cause of many bridge collapse accidents due to vessel, vehicle and other collisions (C. Y. Xia et al. 2012; C. Y. Xia et al. 2014). The factors producing bridge collapses can be divided into two categories: man-made and natural. The man-made factors include design faults, construction mistakes, collisions (by vessels, automobiles and trains), overload, etc. The natural factors include earthquakes, water flow (flood, scouring, etc.), wind, collisions (by floating floes or other objects), environmental deterioration (temperature, corrosion, etc.), etc (C. Y. Xia, Xia et al. 2014). According to importance of trains running safety under vessel-bridge or ice-bridge collision, numerical analyzes and experimental tests have been carried out (C. Y. Xia et al. 2012; C. Xia et al. 2015; Y. Li et al. 2015).

One of the topics that seems to remain silent during the study of railway bridges research background is the lack of consideration of coupled high-speed train and bridge system subjected to wave hydrodynamic load. Many structural failures and vehicle accidents due to extreme wave have been reported in previous studies (Ataei et al. 2010; Kitada 2006; Robertson et al. 2007; Unsworth 2010). Regarding to importance of hydrodynamic failures on coastal bridges, experimental tests for a large-scale bridge superstructure model have been done (Bradner et al. 2011).Wave hydrodynamic lateral force components and vibration may make troubles to the vehicles running on the deck. Also when train crosses over a bridge, asymmetric loading is applied to the bridge which can laterally move the structure. Train moving load on two-lane bridge can cause lateral displacement (Cuadrado et al. 2008). These displacements and accelerations could be increased with the change in wave load and train speed, and may make trouble in riding comfort and running safety according to domestic or international codes' criteria. Many studies have been conducted to determine the amount of wave force applied to marine structures (Chakrabarti 1971; Sorensen 1993; Song 2010). Several analyzes have been carried out in previous studies about coupling hydrodynamic force with other phenomena such as: earthquake, wind, corrosion, scouring, tide level and etc. (Karadeniz 1999; Watanabe and Tomoaki 2003; Eicher, Guan, and Jeng 2003; De-gui et al. 2008; F. Li et al. 2008; Song 2010; S. Yim 2005; Indian Institute of Technology 2010; Wang et al. 2011).

For a bridge, the external load considered in the design may be a vessel collision, an ice-floe collision, a vehicle passing, a train passing, or hydrodynamic loads. However, few of current research studied about considering wave hydrodynamic load on railway bridges. Moreover sometimes more than one of external loads like train passing and wave hydrodynamic load may occur simultaneously. Since various external loads have different properties, the dynamic responses of the bridge and their effects on the running safety of high-speed trains might be different. In this study, running safety means that acceleration and displacement values are allowed regarding to Chinese and European codes in both vertical and lateral directions, which are introduced in next section as railway bridge safety criteria.

In response to this shortage, this article presents a 3D train–bridge–wave (TBW) interaction model. To better study a continuous railway bridge with (32 + 48 + 32) m box girders is considered as an illustrating case study. This bridge is located in China and some research like vessel and ice-floe collision have been carried out which is proper for validation with TBW model (C. Xia et al. 2015; C. Y. Xia et al. 2014). The train used in the validation is selected based on the passing train in the field test (H. Xia and Zhang 2005; Jahangiri and Zakeri 2017).

Most studies carried out in the field of bridge-train interaction are associated with simplifying assumptions like moving load or moving mass. However, considering the importance of high speed railway bridges, these bridges need a higher precision control. In this paper, a two-lane bridge and a high speed train, as well as the interactions between them, are modeled accurately with considering various speeds of train (V). Moreover, in 3D TBW model, hydrodynamic loads with several wave heights (H_s) and periods (T) have been considered according to Morison equation (Sorensen 1993). When hydrodynamic load acts on bridge piers, it may cause dislocation, uneven deformation, displacement or acceleration, which can affect the bridge's response to train passing.

Several scenarios by varying each train speed (V) and wave parameters such as wave height and wave period (H_s, T) have been carried out in this paper. Finally vertical/lateral acceleration (A_y, A_z) and vertical/lateral displacement (U_y, U_z) values of railway bridge deck are compared with the permissible values regarding to Chinese and European codes, and the values of safe and comfort speed according to environmental conditions (wave parameters) are determined in different scenarios.

2 RAILWAY BRIDGE SAFETY CRITERIA

Among the restrictive criteria for safe and comfort passage of high-speed railway bridges are vertical and lateral accelerations and displacements of decks, which have been referred in various sources such as Chinese and European codes. So as mentioned, several scenarios by varying each train speed (V) and wave parameters (H_s, T) have been carried out in this paper. Finally vertical/lateral acceleration (A_y, A_z) and vertical/lateral displacement (U_y, U_z) values of railway bridge are compared with the permissible values regarding to Chinese and European codes (CEN 2005a, 2005b, 2005c; China 2009; Jeon et al. 2016), and the values of safe and comfort speed according to sea states (wave parameters) are determined in these scenarios.

2.1 China's High-Speed Railway Bridges Criteria

China's high-speed railway bridges criteria for displacement and acceleration, which have been used to study safe and comfort passing in this study (China 2009), are as follows:

a) The maximum allowable vertical displacement of the deck is determined by Table 1 for different speeds.

Table 1-Maximum Allowable Vertical Displacement of Bridge

Range of Span / Designed Speed	L ≤ 40 m	40 m < L ≤ 80 m	L > 80 m
250 km/h	L/1400	L/1400	L/1000
300 km/h	L/1500	L/1600	L/1100
350 km/h	L/1600	L/1900	L/1500

b) The maximum allowable lateral displacement of the deck (U_z) is determined by Equation 1 according to length of span (L).

$$U_z \leq \frac{L}{4000} \tag{1}$$

c) The maximum vertical and lateral acceleration of the deck (A_y, A_z) are determined as 0.13g and 0.1g, respectively.

Also for better review, another codes such as European codes and ISO criteria have been used to study safe and comfortable passing in this study.

2.2 European's High-Speed Railway Bridges Criteria

a) According to Euro Codes, the maximum allowable vertical displacement of the deck (δ) is determined by figure 1.

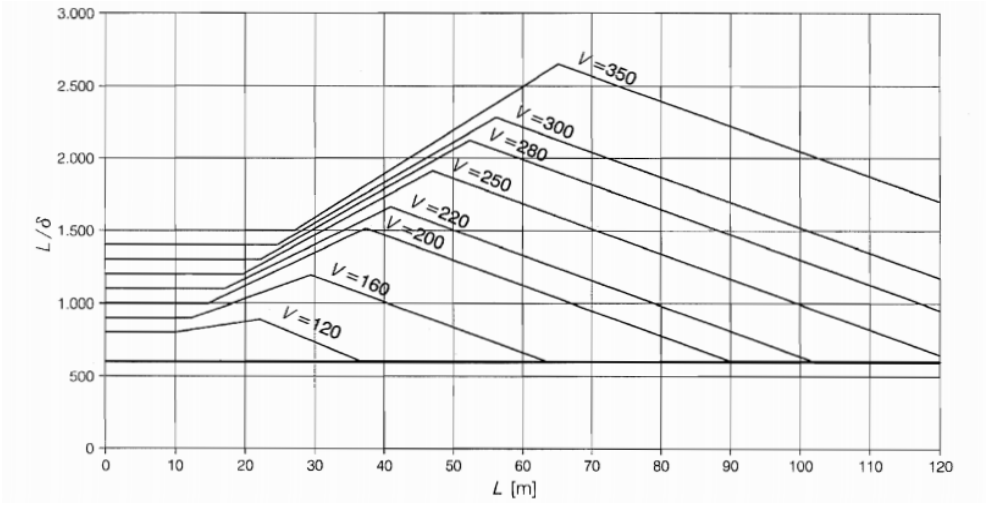


Figure 1- *Maximum Allowable Vertical Displacement of Bridge* (Bouassida et al. 2012; CEN 2005a, 2005b)

b) According to Euro Codes, the maximum allowable lateral displacement of the deck (U_z) is determined by Equation 2 according to length of span (L) and maximum allowable horizontal rotation ® as shown in Table 2.

$$U_z \leq \frac{L^2}{8*r} \tag{2}$$

Table 2- *Maximum Allowable Lateral Displacement of Bridge* (Bouassida et al. 2012; CEN 2005a, 2005b)

Speed (km/h)	Single Deck	Multi Deck Bridge
V ≤ 120	r_1	r_4
120 < V ≤ 200	r_2	r_5
V > 200	r_3	r_6
	r_1=1700, r_2=6000, r_3=14000	
	r_4=3500, r_5=9500, r_6=17500	

c) According to Euro Codes and ISO, the maximum vertical and lateral acceleration (A_y, A_z) are determined as 1.25 m/s^2 for the good safety and comfortable train passing on bridge (Jeon et al. 2016; ISO 2002; Jiang et al. 2019; CEN 2005a, 2005b).

Comparing the two codes with each other, it can be seen that in general, the Chinese code offers more restrictive criteria than the European codes. However, both codes have been used to better investigate the present research outcomes in the next sections.

3. INTERACTION MODELS DEVELOPMENT

3.1 Train-Bridge Interaction Model

The China high-speed train and bridge models are used in this study. A 3D FE model is employed in Abaqus finite element software to model and analyze the bridge and train while considering the interaction between them using the Hertz theory (Bhaskar et al. 1997). Next, Abaqus model is validated by comparing the lateral acceleration of bridge under vessel collision load which is done by (C. Y. Xia et al. 2014). The 3D Train-Bridge-Wave model (TBW) is then used to assess sensitivity analysis according to wave height (H) and train speed (V) variations to monitoring train riding comfort and running safety according to code's criteria.

The train model is composed of locomotive and wagon. Each locomotive or wagon consists of a car body, two bogies, four wheel-sets, and the spring and damping connections between the three components. The car body configuration and train's mechanical properties and dimensions are presented according to china high speed train in Figure 2 and Table 3, respectively. Also, cross section of the concrete box deck is illustrated in Figure 3.

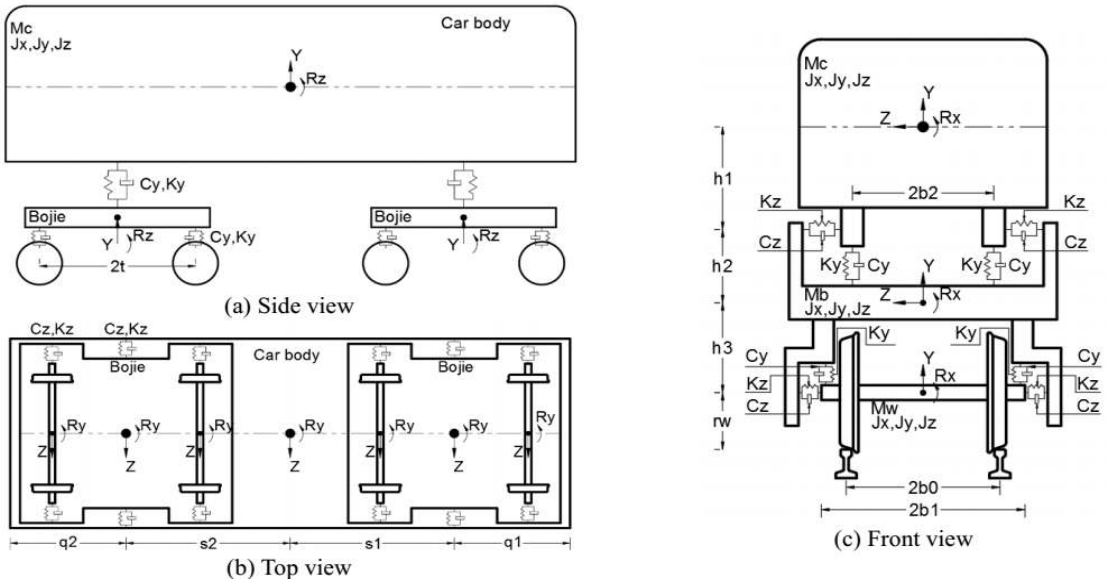


Figure 2- Car body configuration

Table 3- Train's Mechanical Properties and Dimensions

DESCRIPTION	NAME	UNIT	POWER CAR	PASSENGER CARS
CAR-BODY DIMENSIONS	s1; s2; q1; q2; h1	m	5.73;5.73;6.8;3.75;0.75	9;3.75;3.75;0.75
MASS OF CAR-BODY	Mc	ton	63.98	43.82
CAR-BODY INERTIA MOMENTS	Jx; Jy; Jz	ton.m2	59.4; 2505.3; 2485.4	23.2; 2100; 2080
MASS OF BOGIE	Mb	ton	3.434	3.04
BOGIE INERTIA MOMENTS	Jx; Jy; Jz	ton.m2	1.766; 2.453; 4.905	1.580; 2.344; 3.934
SECONDARY SUSPENSION STIFFNESS	Kz; Ky	KN/m	297.2; 1245.87	176; 265
SECONDARY SUSPENSION DAMPING	Cz; Cy	KNS/m	98.1; 98.1	39.2; 45.12
SECONDARY SUSPENSION DIMENSIONS	b2; h2	m	1.23; 0.42	1.23; 0.42
PRIMARY SUSPENSION STIFFNESS	Kz; Ky	KN/m	2452.5; 1226.25	2350; 590
PRIMARY SUSPENSION DAMPING	Cz; Cy	KNS/m	98.10; 29.43	58.86; 19.62
MASS OF WHEEL-AXLE	Mw	ton	1.776	1.776
WHEEL-AXLE MOMENT	Jx; Jy; Jz	ton.m2	1.138; 1.138; 0.00785	1.138; 1.138; 0.00785
PRIMARY SUSPENSION & WHEEL	b0; b1; h3; t; rw	m	0.75; 1; 0.2; 1.25; 0.455	0.75;1;0.2;1.25;0.455

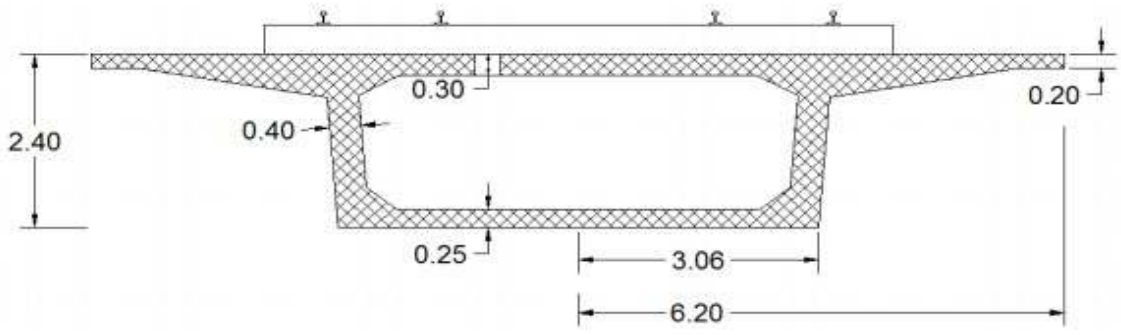


Figure 3- Cross Section of the Concrete Box Deck

For a simplified though still accurate enough analysis, the following assumptions are made in modeling the train vehicle:

(1) The car body, bogies and wheel-sets in each vehicle are regarded as rigid components, neglecting their elastic deformation during vibration as shown in Figure 4.

(2) The connections between car body, bogies and wheel-sets are represented by linear springs and viscous dashpots (as shown in Figure 5 and 6).

(3) Each train body has five degrees-of-freedom (DoFs). They correspond to the lateral displacement, the roll displacement, the yaw displacement, the vertical displacement, and the pitch displacement. Each bogie on the vehicle has five DoFs: the lateral displacement, the roll displacement, the yaw displacement, the vertical displacement, and the pitch displacement. For each wheel under the bogie, three DoFs are considered: the lateral displacement, the roll displacement, and the vertical displacement. Thus the train is modeled in TBW for each vehicle with 2-bogies and 4-axles can be modeled by a 27-dof dynamic system, as shown in figure 6.

(4) Regarding to other research (Rashid 2011), in longer spans (L >15m) the dynamic response is not sensitive to track stiffness value, so slab track is not modeled separately and merged with deck as an integrated model. Piers and deck are modeled as 3D deformable solid element with considering concrete specification. Rails are modeled as 3D deformable solid element with considering steel specification and tied on deck, also for considering the interaction between wheels and rails the Hertz theory is used (as shown in figure 5 and 6).

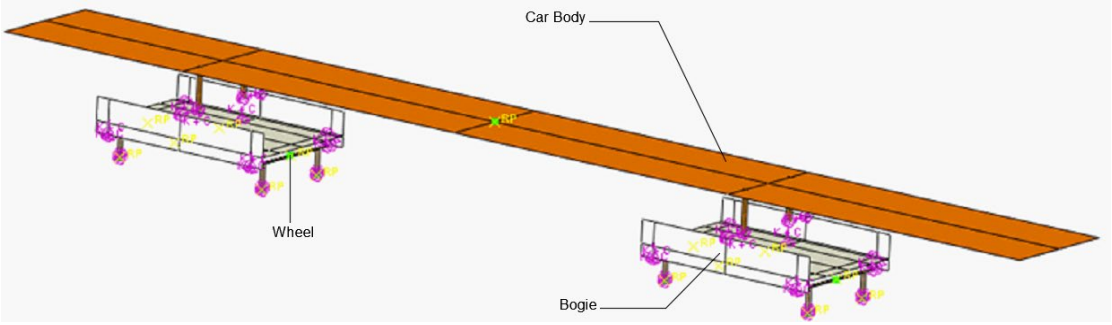


Figure 4- Train 3D Model

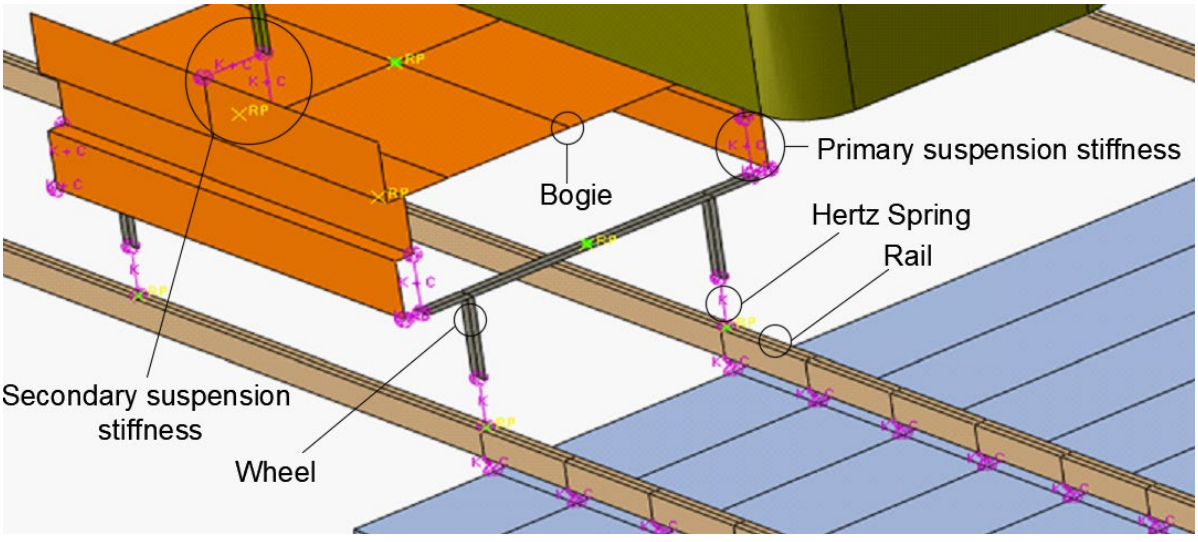


Figure 5- Modeling Wheel-Rails Interaction by Hertz Spring

(5) The considered bridge is a two-lane continuous with concrete box (32+48+32) m (as shown in Figure 6). The substructure of the bridge includes four concrete solid piers with rectangular sections (8m x 4.5m) and piers are fixed at seabed. Deck mounted on piers are fixed pot neoprene bearings and the bearings are modeled according to the design (C. Y. Xia et al. 2014). For the fixed bearings, the rotational angle about the transverse axis z of the girder end is free, while the other 3 translational displacements and 2 rotational angles are connected through master-and-slave relations to the pier-top and the damping ratio of the bridge is taken as 2.5%. The height of piers

are assumed 20 m and sea level which is proposed hydrodynamic force interaction with piers is considered at level +15m.

(6) Train passes the bridge with different speeds (200 to 400 km/h) applied to sensitivity analysis.

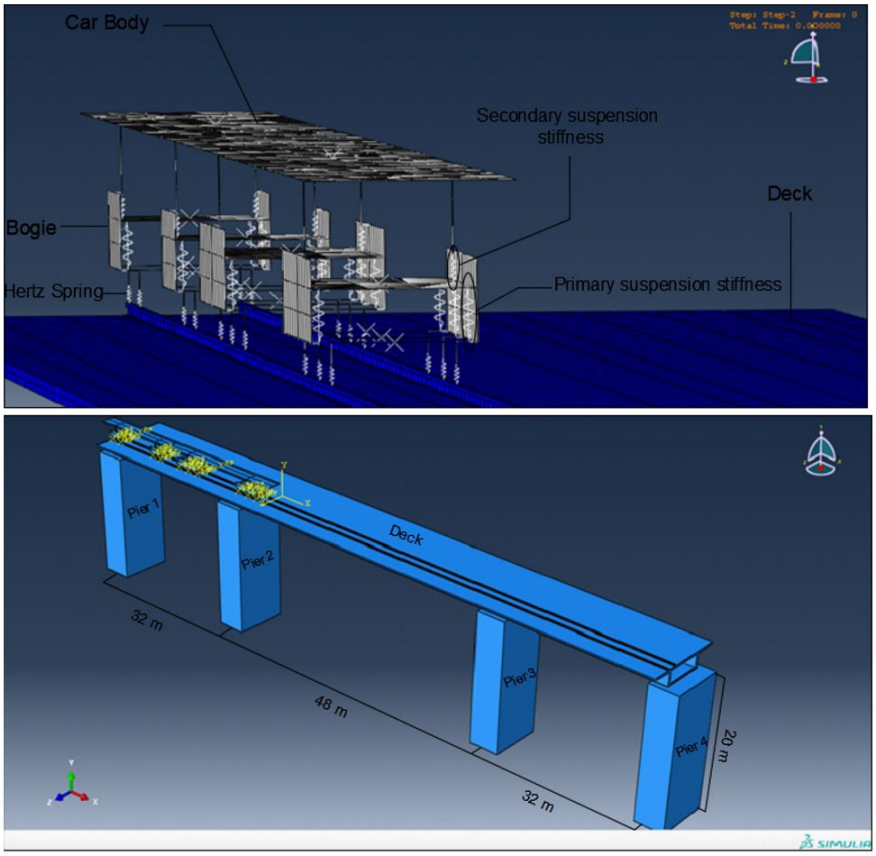


Figure 6- Train-Bridge 3D Model

Summary of the train modeling method and the definition of its interaction with the bridge is provided in the following steps:

A) Several 3D models were developed in real dimensions of car-body, bogies and wheels by using 3D discrete rigid shells module in Abaqus.

B) Real mass and inertia were assigned for each part of wagon and locomotive according to car-body's specification (which are represented in table 3).

C) Several springs were modeled to connect different parts of car-body to each other by using interaction module of Abaqus. In this model several rigid parts were linked in all directions by primary and secondary springs for considering suspension stiffness and damping (as shown in figure 3 and 4).

D) All wheels were connected to rails by using interaction module of Abaqus and applying hertz theory.

E) In addition to define displacement and rotation boundary conditions, velocity boundary condition in x direction was defined to model car-body movement in Abaqus to perform dynamic analysis.

3.2 Hydrodynamic Force on Pier

Based on the Morison's potential fluid theory (Sorensen 1993), it is assumed that the effect of fluid on the structure is caused by the acceleration field and velocity field, and the effect of structure on the movement of fluid could be ignored. Therefore, the hydrodynamic force (F_{Wave}) acting on the column includes two components (as shown in Eq.3-6): one is the inertial force (F_I) and the other is the drag force (F_D) on the column due to the effect of viscous and swirl (as shown in Figure 7).

Morison equation is adopted to calculate the wave forces on the columns, of which the structure diameter or width D is smaller than 0.2 times wave length L.

$$F_{Wave} = F_D + F_I \tag{3}$$

$$F_D = \frac{C_d}{2} \rho A u^2 \tag{4}$$

$$F_I = C_m \rho V \dot{u} \tag{5}$$

$$F_{Wave} = \frac{C_d}{2} \rho A u^2 + C_m \rho V \dot{u} \tag{6}$$

Here, ρ is the density of the fluid, V is the volume of the submerged structure, A is the area of the column section, u and $\dot{u}$ are the absolute velocity and acceleration of the fluid respectively, C_m is the inertia coefficient and C_d is the drag force coefficient of the fluid. The total hydrodynamic force on the unit length (ds) of the column along the Z-axis direction can be expressed as:

$$F_{Hydrodynamic} = \frac{F}{ds} = \frac{C_d}{2} \rho D u^2 + C_m \rho \left(\frac{\pi D^2}{4}\right) \dot{u} \tag{7}$$

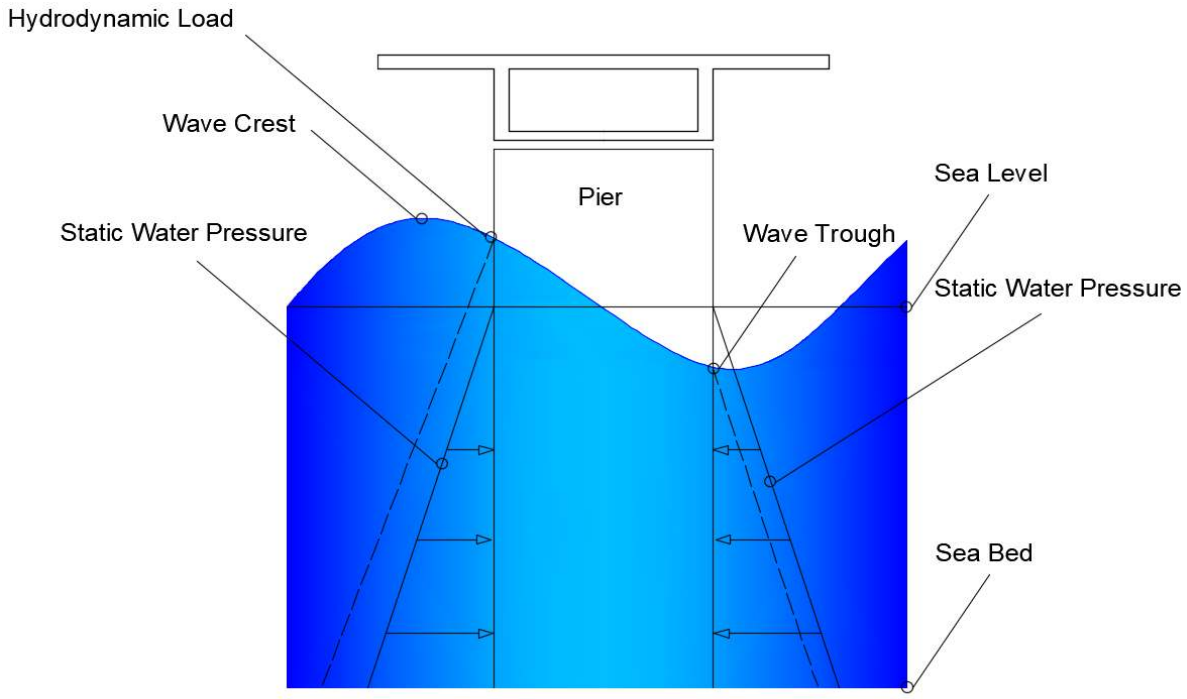


Figure 7- Hydrodynamic Force on Pier

The China Sea experiences severe typhoon impact every year. That also cause extreme wind waves (Cao et al. 2018). The estimate of extreme wave height is of great importance for human activities in China Sea. Since the generation of typhoon is still unpredictable, it is very difficult to estimate the storm waves. Currently, many researcher have studied the extreme wave parameters of the China Sea. In this paper, wave height and period are estimated by using local wind speed, fetch length and wind duration (as shown in Table 4).

Table 4- *Wave Estimation According to Wind Conditions* (Cao et al. 2018)

Wind Conditions			Wave Size		
Wind Speed in One Direction	**Fetch**	**Wind Duration**	**Average Height**	**Average Wavelength**	**Average Period**
56 km/h	518 km	23 h	4.1 m	76.5 m	8.6 sec
74 km/h	1313 km	42 h	8.5 m	136 m	11.4 sec
92 km/h	2627 km	69 h	14.8 m	212.2 m	14.3 sec

Three sea states, sea states I, II, and III, are considered based on three different mean wind speeds U_{Wind} of 56, 74, and 92 km/hr for China Sea area. The characteristics of selected sea states for TBW model are defined in Table 5.

Table 5- Selected Sea States for TBW Model

Sea States	H_s(m)	T_s(s)
I	4.1	8.6
II	8.5	11.4
III	14.8	14.3

The wave hydrodynamic force is calculated and applied to the Abaqus model as harmonic forces according to the marine conditions as mentioned in Table 5 and Equation 7. The assumed values for the coefficients C_d and C_m are 1 and 2, respectively (Chakrabarti 1971; Sorensen 1993; Song 2010).

3.3 Train - Bridge – Wave Model

As mentioned previously, wave hydrodynamic lateral force could make troubles to the trains running on the deck. Also when train crosses over a bridge, asymmetric loading is applied to the bridge which can move the structure (as shown in Figure 8). The wave hydrodynamic force is calculated and applied to the Abaqus train-bridge-wave model (TBW) according to the marine conditions mentioned in Table 5 and using Equation 7. Vertical and lateral displacements and accelerations could be increased with the change in wave load and train speed, and may make trouble in riding comfort and running safety according to code's criteria.

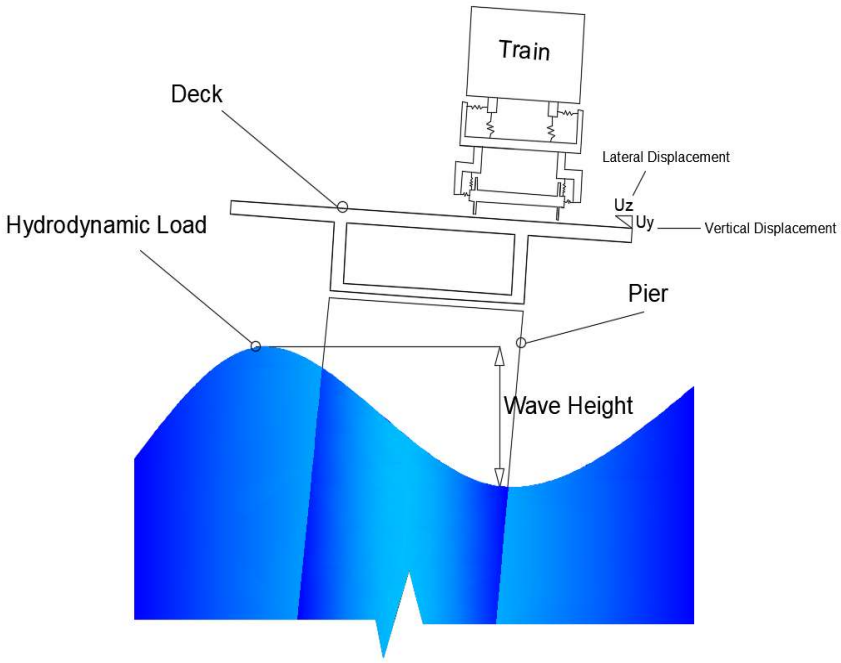


Figure 8- Pier Lateral Movement Due To Wave Force

Bridge, Train and Hydrodynamic load modeling are performed using the FEM in Abaqus software. Sea states I, II, and III, are applied to assess sensitivity analysis. As mentioned, substructure of the bridge includes four concrete solid piers with rectangular sections (8m x 4.5m) and piers are fixed at seabed. The height of piers are assumed 20 m and sea level which is proposed for hydrodynamic force interaction with piers is considered at level +15m. The wave direction (Z-axis) is assumed to be perpendicular to the train passing direction (X-axis). Also, hydrodynamic load is applied to bridge piers simultaneously and train passes the bridge with different speeds (200 to 400 km/h) to sensitivity analysis. Fifteen scenarios with wave and train speed variation have been applied in this study. Also additional analyses for considering effect of presence or absence of wave for train running on bridge are performed. Full 3D Train-Bridge-Wave (TBW) model is shown in Figure 9. As mentioned, China high speed railway code and European code are used for assess riding comfort and running safety. In order to make a good judgment with respect to the importance of wave reaching time to the piers, as the worst scenario each maximum value of hydrodynamic loads are applied on piers at the time when the train arrives middle of deck.

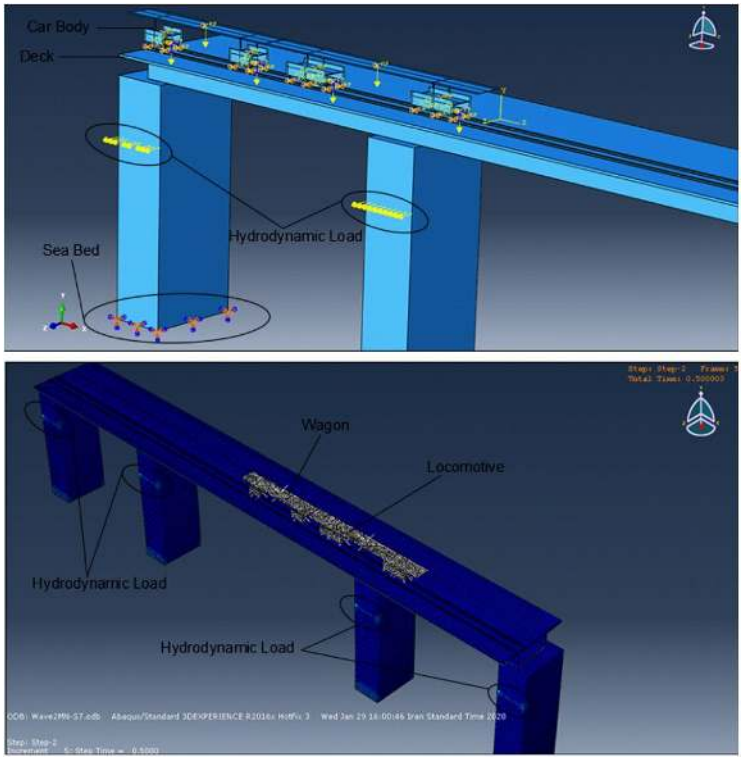


Figure 9- Train-Bridge-Wave (TBW) 3D Model

Train-bridge-wave modeling is presented by a flowchart as shown in Figure 10 to show the solving methodology.

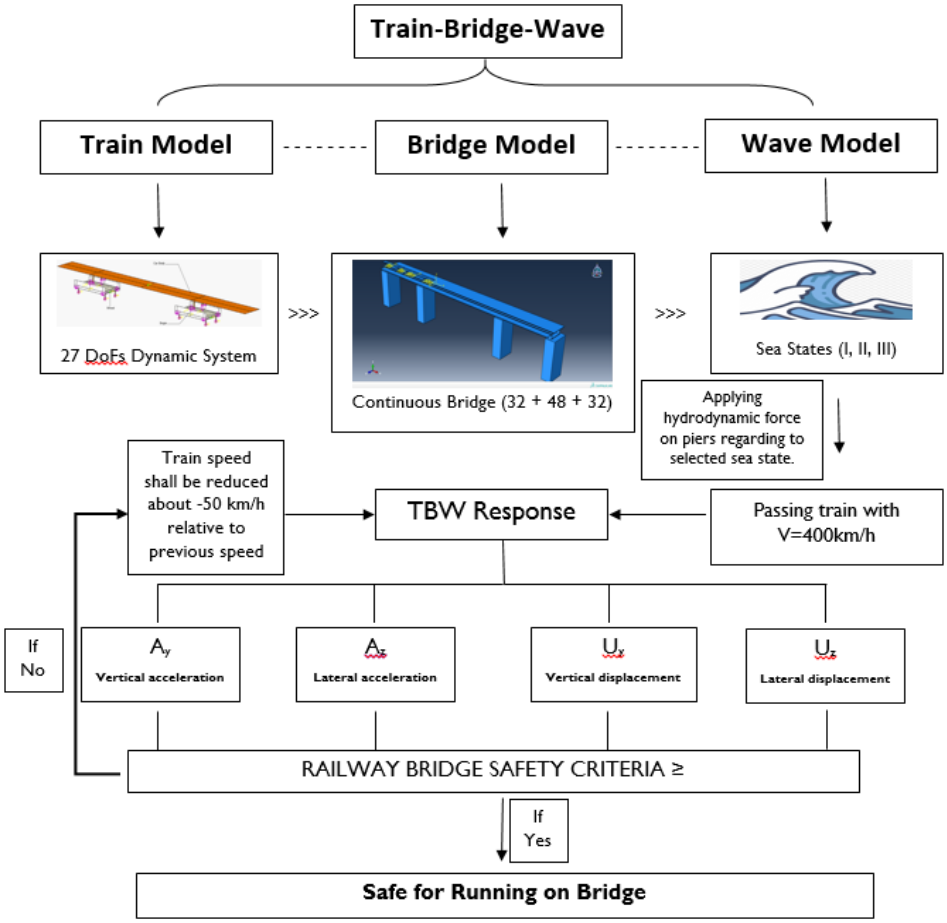


Figure 10- Train-Bridge-Wave Solving Methodology

3.4 Model Validation

The 3D finite element model of Train-Bridge-Wave was validated according to numerical simulation results of Train-Bridge model with considering 10 MN vessel collision load which is applied on pier 2 at level +10 m above the seabed. The vessel load is taken from reference (C. Y. Xia et al. 2014) and represents the collision history by a ship, which is a wide continuous pulse with the total duration of 1.8 s, as shown in Figure 11.

The equations of motion for the train–bridge system subjected to a collision load can be expressed as:

$$\begin{bmatrix} M_{VV} & 0 \\ 0 & M_{BB} \end{bmatrix} \begin{Bmatrix} \ddot{x}_V \\ \ddot{x}_B \end{Bmatrix} + \begin{bmatrix} C_{VV} & C_{VB} \\ C_{BV} & C_{BB} \end{bmatrix} \begin{Bmatrix} \dot{x}_V \\ \dot{x}_B \end{Bmatrix} + \begin{bmatrix} K_{VV} & K_{VB} \\ K_{BV} & K_{BB} \end{bmatrix} \begin{Bmatrix} x_V \\ x_B \end{Bmatrix} = \begin{Bmatrix} F_{VB} \\ F_{BV} \end{Bmatrix} + \begin{Bmatrix} 0 \\ F_C \end{Bmatrix} \tag{8}$$

Where M, C and K are mass, damping and stiffness matrices of the train–bridge system, x, ẋ and ẍ are displacement, velocity and acceleration vectors, respectively; F_{VB} and F_{BV} are interaction forces between vehicle and bridge, and the subscripts V and B represent vehicle and bridge, respectively. The components of these matrices and vectors can be found in reference (C. Y. Xia et al. 2014) . F_C is the generalized vector of the collision load applied on the bridge.

In the validation stage, the train consists of wagons and locomotives with considering vessel collision load is modelled as shown in Figure 12, and lateral acceleration time histories comparison at the top of pier 2 under vessel collision load for a train speed of 200 km/h is presented as Figure 13. In the sensitivity analysis, the train consists of one locomotive and one wagon. The axle loads of locomotive and wagon are 19.5 and 14.25 tons, respectively. Dimensions and mechanical properties of the train car (27-DOFs dynamic system) are described in Figure 2 and Table 3. Vessel impact is modeled as concentrated loads which are distributed on contact level of vessel and pier 2, as shown detailed in Figure 12. Mesh size is one of the effective parameters in FEM analyses. Mesh configuration can be selected regarding to several conditions. Although smaller elements lead to a higher precision of the model, they require more time to analyze. In this research, several analyses are carried out with various mesh sizes on the bridge model to determine the optimum meshing dimensions. Results did not experience any recognizable changes by decreasing the mesh sizes smaller than 0.5 m. Consequently in this study, optimal mesh size is selected 0.5 m as shown in Figure 12 to obtain proper train, rail and deck interactions. Moreover choosing this mesh size is helpful about including rail and deck connection points. The comparison with numerical study demonstrated that the results of the present model were close to collision test results. The adjustment of the results of the two models is higher than 92% for maximum values comparison and 87% for root mean square comparison as shown in Figure 13. These 8% and 13% differences for maximum and RMS values could be due to some of the simplifications considered in the train-bridge interaction model, input parameters and modeling errors, calculation methods and etc. In this study, time step is taken as 0.005 s. Xia et al. (2014) considered this parameter as 0.0001 s in their numerical analysis. This subject is one of the main reasons for 13% difference between the results of present study and Xia et al. (2014) results.

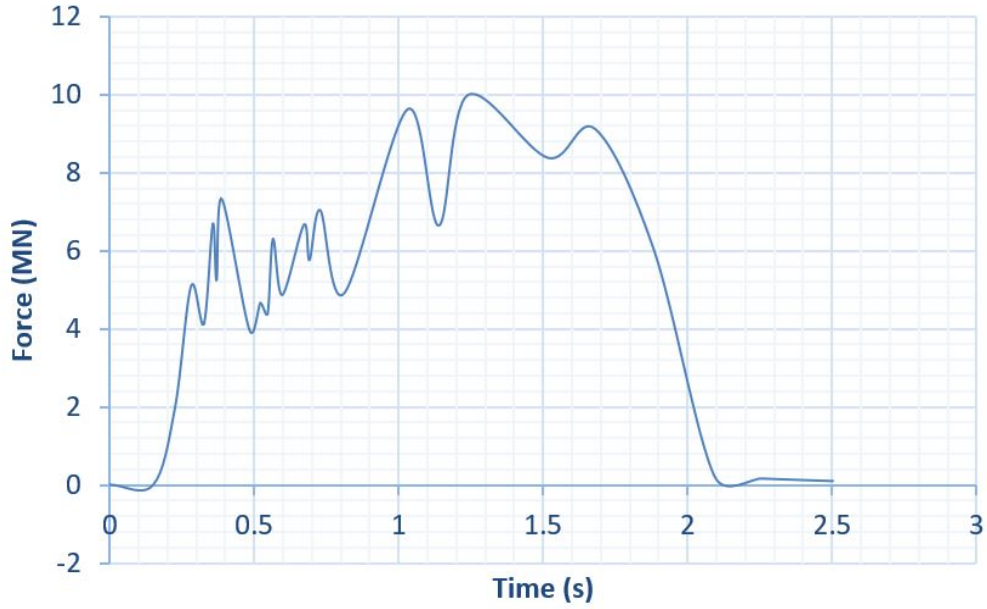


Figure 11- Time Histories of Vessel Collision Load

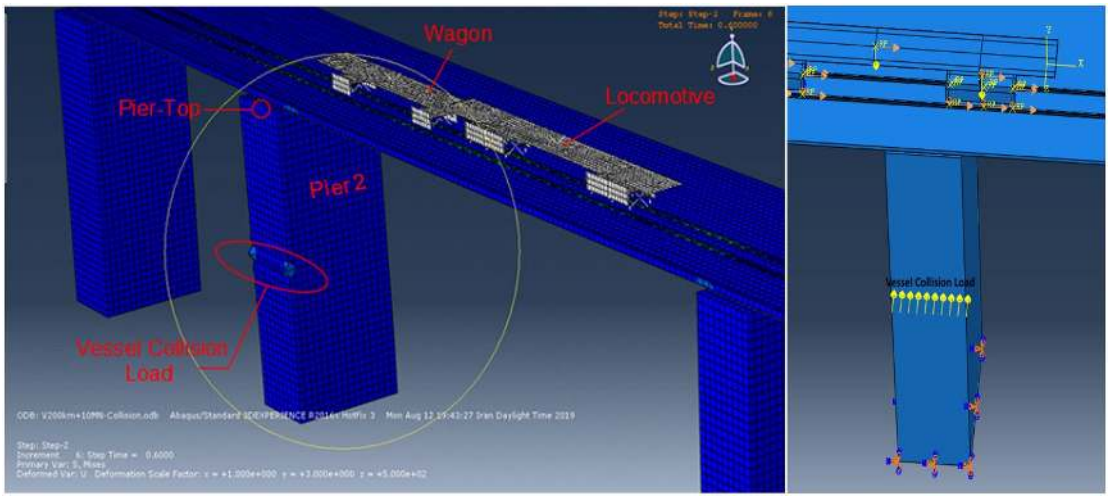


Figure 12- 3D Validation Model for Considering Vessel Collision Load

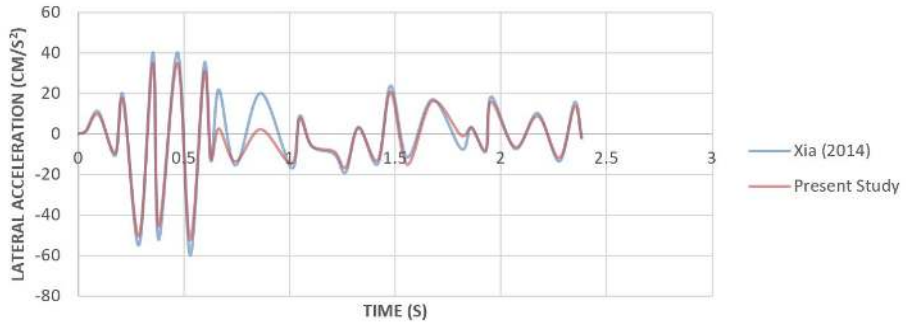


Figure 13 – Comparing Lateral Acceleration Time Histories at the Top of Pier 2 under Vessel Collision Load for a Train Speed of 200 km/h

4. SENSITIVITY ANALYSES

By using this 3D validated model, some important parameters effects on the running safety of high-speed train on a bridge subjected to hydrodynamic load can be assessed. In this study, several scenarios as shown in Table 6 are applied according to assuming various train speeds and sea states. Moreover, other extra analyses are simulated with and without hydrodynamic force for a train speed of 300 km/h. In all cases with hydrodynamic force, the time history of the sea states are applied on piers at level +15 m above the seabed.

Table 6- Scenarios for Wave and Train Speed Variation

Scenario	Speed (km/h)	H_s(m)	T_s(s)
1	200	4.1	8.6
2	200	8.5	11.4
3	200	14.8	14.3
4	250	4.1	8.6
5	250	8.5	11.4
6	250	14.8	14.3
7	300	4.1	8.6
8	300	8.5	11.4
9	300	14.8	14.3
10	350	4.1	8.6
11	350	8.5	11.4
12	350	14.8	14.3
13	400	4.1	8.6
14	400	8.5	11.4
15	400	14.8	14.3

5. Sensitivity Analyses of TBW Model under Several Conditions

This section investigates the dynamic response of bridge during the train passes with several speeds through the bridge under several sea states by time history analyses. Structural dynamic response discussed in this study includes the lateral displacement (U_z), vertical displacement (U_y), lateral and vertical acceleration (A_z, A_y) response at the middle point of span. The performance of bridge structure and train (TBW model) under different sea states and speeds is carefully discussed.

5.1 The Effect of Hydrodynamic Load on Railway Bridge

First, to study the effect of the waves on the safety of the bridge to train passing, analyzes are simulated with and without hydrodynamic loads. And the bridge's behavior, such as: vertical and lateral displacements and accelerations are compared when the train passes at a speed of 300 km / h.

As shown in Figure 14, when train is passing on bridge without hydrodynamic force (wave height=0), the amount of lateral displacement under train passing (which is less than 1 mm) is less than the permissible value. In the following, by applying hydrodynamic loads on piers and increasing the height of the wave, the lateral displacement of the deck increases and exceeds the permissible values of the European and Chinese codes.

Lateral displacement response of the bridge subjected to stormy hydrodynamic load (H = 14.8 m) could be up to 26 times higher than the ones without hydrodynamic load.

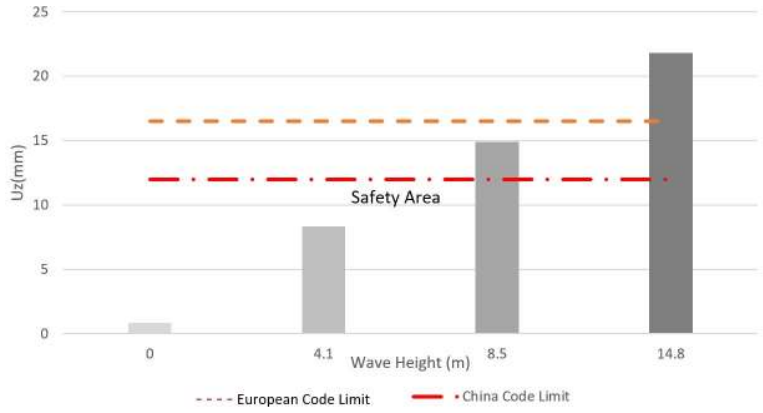


Figure 14- Lateral Displacement of the Bridge Deck against Several Sea States *(Train speed: 300 km/h)*

As shown in Figure 15, by applying hydrodynamic loads on piers and increasing the height of the wave, the vertical displacement of the deck increases but do not exceeds the permissible values of the codes. However, due to the increasing trend of displacement with increasing wave height, the displacement will be approached to critical values. (Negative value indicates downward vertical displacement)

Vertical displacement response of the bridge subjected to stormy hydrodynamic load (H = 14.8 m) is 40% higher than the ones without hydrodynamic load.

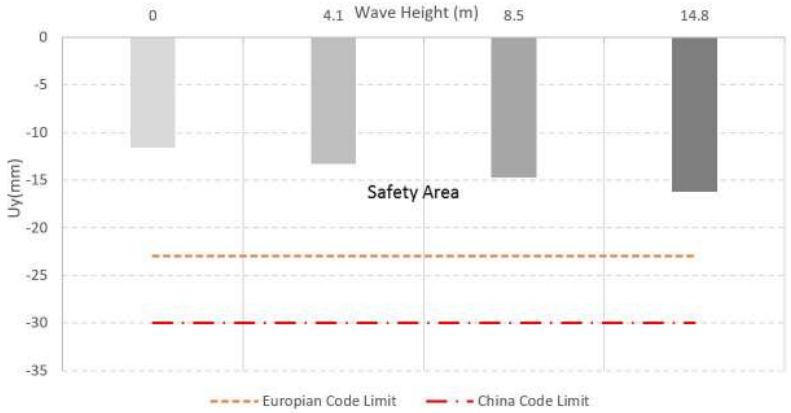


Figure 15- Vertical Displacement of the Bridge Deck against Several Sea States *(Train speed: 300 km/h)*

When train is passing on bridge without hydrodynamic force (wave height=0), the amount of lateral acceleration under train passing is less than the permissible value (which is negligible). By applying hydrodynamic loads on piers and increasing the height of the wave, the lateral acceleration of the deck increases and exceeds the permissible values of the European and Chinese codes (as shown in Figure 16).

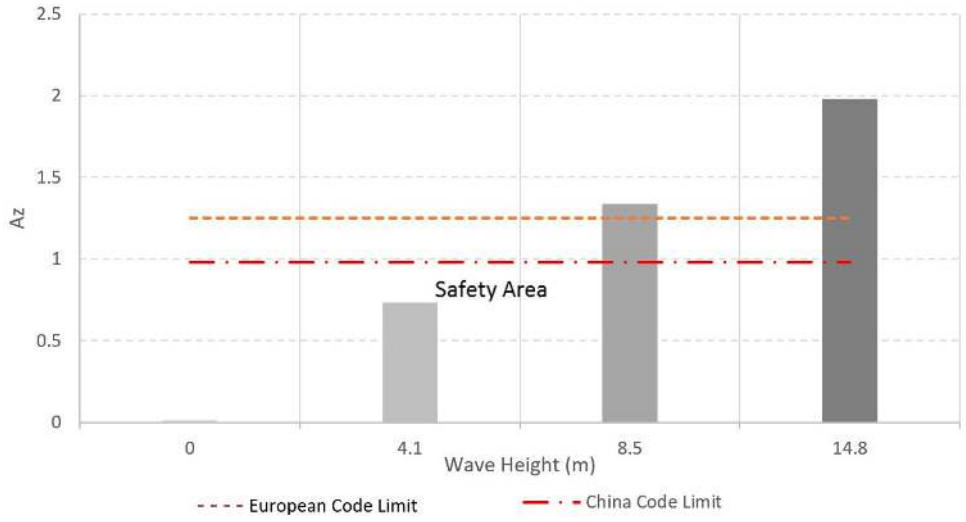


Figure 16- Lateral Acceleration (M/S2) of the Bridge Deck against Several Sea States (Train speed: 300 km/h)

As shown in Figure 17, when train is passing on bridge without hydrodynamic force (wave height=0), the amount of vertical acceleration under train passing is 0.8 m/s^2, which is less than the permissible value. In the following, by applying hydrodynamic loads on piers and increasing the height of the wave, the vertical acceleration of the deck increases and exceeds the permissible values when wave height exceeds 8 m. Also, the intensity of the acceleration has increased after the 4.1-meter wave, which indicates that after this wave height, the bridge will be more sensitive to changes.

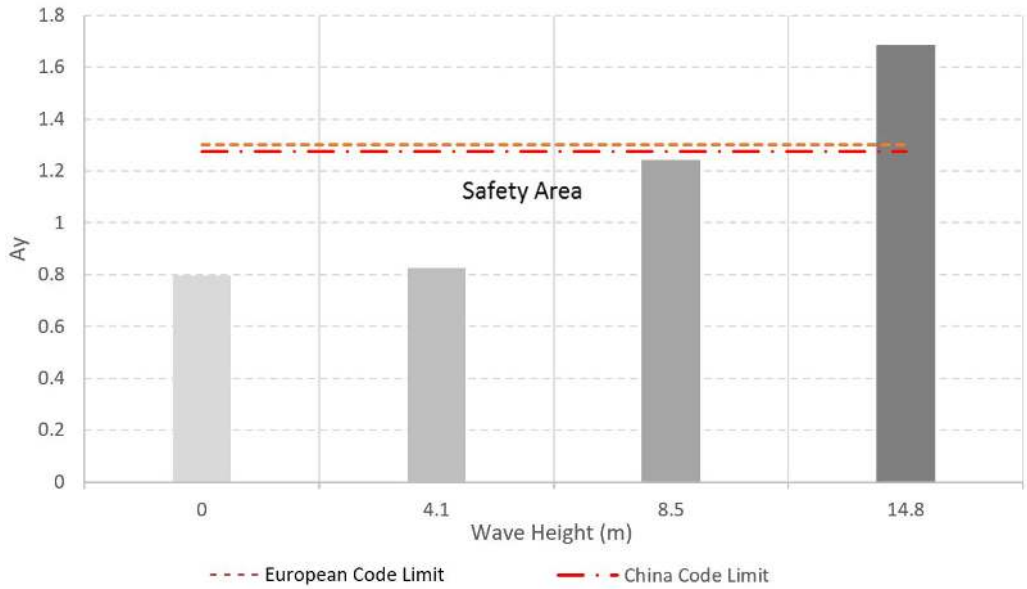


Figure 17- Vertical Acceleration (M/S^2) of the Bridge Deck against Several Sea States *(Train speed: 300 km/h)*

5.2 TBW Model under Several Sea States and Train Speeds

In this section, sensitivity analyzes of TBW model are carried out and discussed under several train speeds in different sea states. Sea states as shown in Table 2 are used in this study and responses under different train speeds (200,250,300,350 and 400 km/h) are provided. Figures 18, 19, 20 and 21 show diagram trends according to speed change and figures 22, 23, 24 and 25 show diagram trends according to wave height change.

As shown in Figure 18, for the sea-state I, lateral displacements are permissible according to both China and European codes. For the sea-state II, lateral displacements are permissible according to European code but impermissible according to China code. And for the sea-state III, lateral displacements are impermissible according to both of codes. Also lateral displacements for upper sea-states are greater than lower sea-states.

As shown in Figure 19, for all scenarios, vertical displacements are permissible according to both China and European codes. However vertical displacements for upper sea-states are greater than lower sea-states and due to the increasing trend of displacement with increasing wave height, it is possible to be critical at higher wave heights. It is also worth noting that by changing the speed, the permissible values will also change according to the codes. (Negative value indicates downward vertical displacement)

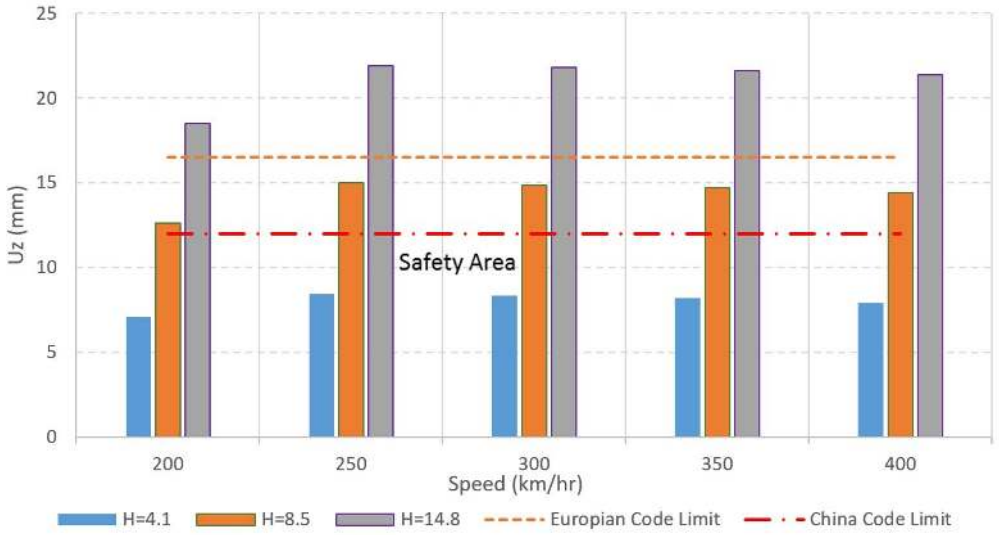


Figure 18- Lateral Displacement of the Bridge Deck under Different Train Speeds for Several Sea States

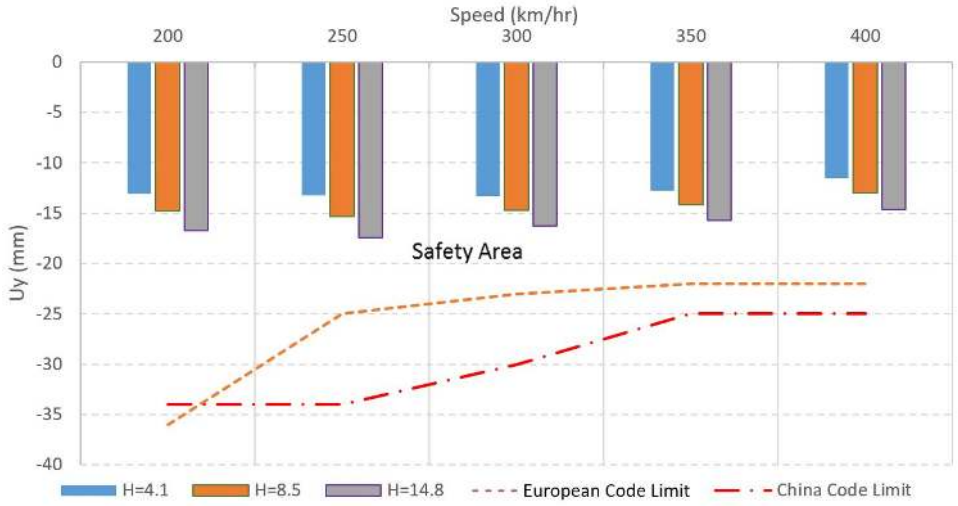


Figure 19- Vertical Displacement of the Bridge Deck under Different Train Speeds for Several Sea States

As shown in Figure 20, for the sea-state I, lateral accelerations are permissible according to both of China and European codes. For the sea-states II and III, lateral accelerations are permissible for speed less than 250 km/h, but for speeds more than 250 km/h, responses are impermissible. Also lateral accelerations for upper sea-states are greater than lower sea-states.

Moreover, the present study provides some other useful outputs. As shown in figure 20 response for scenario 5 (V=250 km/h, H=8.5m) is impermissible and higher than response of scenario 3 (V=200 km/h, H=14.8m) and scenario 4 (V=250 km/h, H=4.1m) which are permissible. This output indicates that in stormy conditions, the speed of the train crossing the bridge should be reduced, or train should be waited on calmer sea-state according to weather forecast.

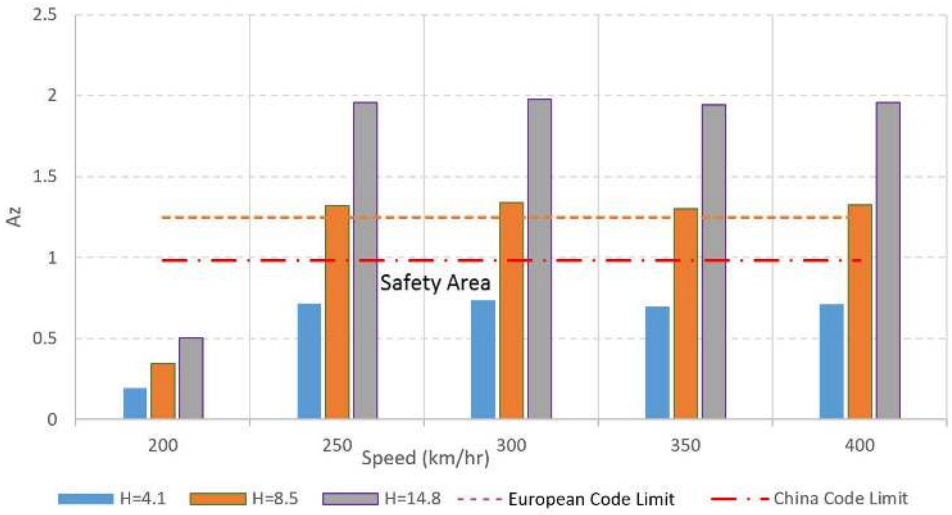


Figure 20- Lateral Acceleration (M/S^2) of the Bridge Deck under Different Train Speeds for Several Sea States

As shown in Figure 21, for the sea-state I, vertical accelerations are permissible according to both codes. For the sea-states II, by increasing the train speed, the vertical acceleration of the deck increases and closes to impermissible line. For the sea-states III, by increasing the train speed, the vertical acceleration of the deck increases and exceeds the permissible values when train speed exceeds 250 km/h. Also, vertical accelerations for upper sea-states are greater than lower sea-states.

Moreover, as shown in Figure 21, response for scenario 3 (V=200 km/h, H=14.8m) is less than response of scenario 14 (V=400 km/h, H=8.5 m). This output indicates that in stormy conditions, the speed of the train crossing the bridges should be reduced for safe and comfortable passing.

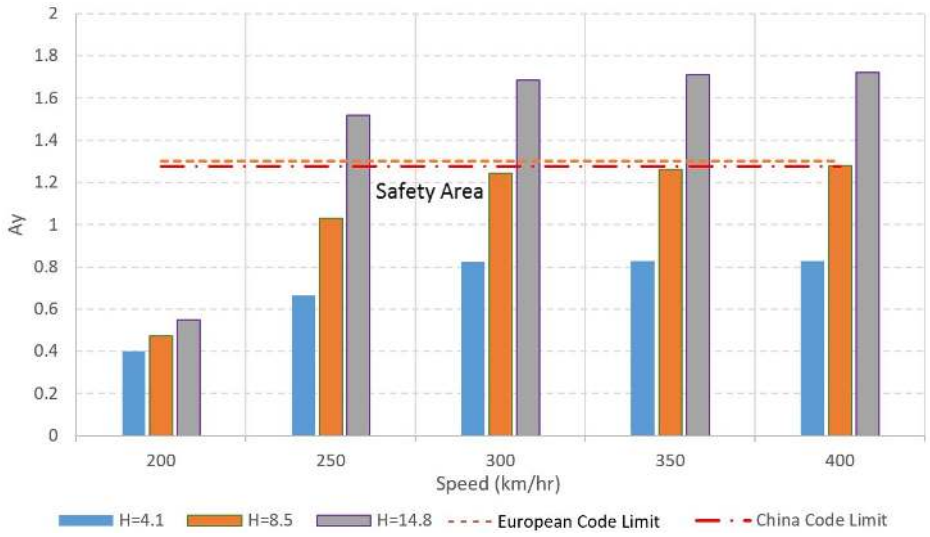


Figure 21- Vertical Acceleration (M/S^2) of the Bridge Deck under Different Train Speeds for Several Sea States

As shown in Figure 22, by applying hydrodynamic loads on piers and increasing the height of the wave, the lateral displacement of the deck increases and exceeds the permissible values of the codes. All outputs are permissible for sea-state I and all of them are impermissible for sea-state III. So, results show the importance of sea conditions for safe and comfortable train passing on bridge. Also for lateral displacement, the most increase is observed between 200 km/h and 250 km/h and other speeds have similar trend to 250 km/h. Lateral displacement may not decrease considerable when train speed decreases from 400 km/h to 250 km/h, and train speed shall be reduced under 250 km/h for safe and comfortable passing.

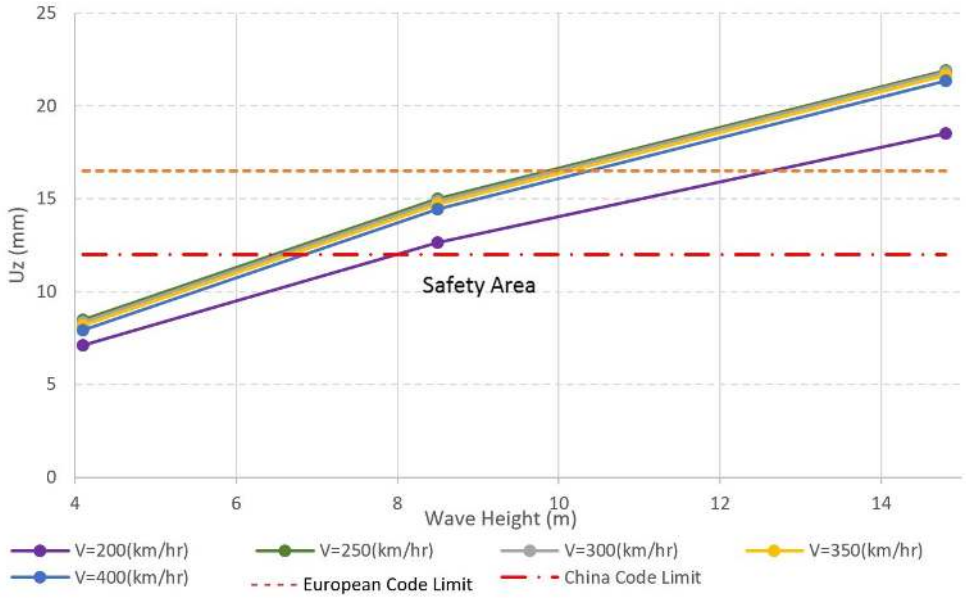


Figure 22- Response of Lateral Displacement under Train Speeds for Several Wave Height

As shown in Figure 23, by applying hydrodynamic loads on piers and increasing the height of the wave, while the vertical displacement of the deck increases but it not exceeds the permissible values of the codes. However, due to the increasing trend of displacement with increasing wave height, the displacement value may become critical at higher wave heights and speeds. Also for vertical displacement same as lateral displacement, the most increase is observed between 200 km/h and 250 km/h and other speeds are among them. (Negative value indicates downward vertical displacement)

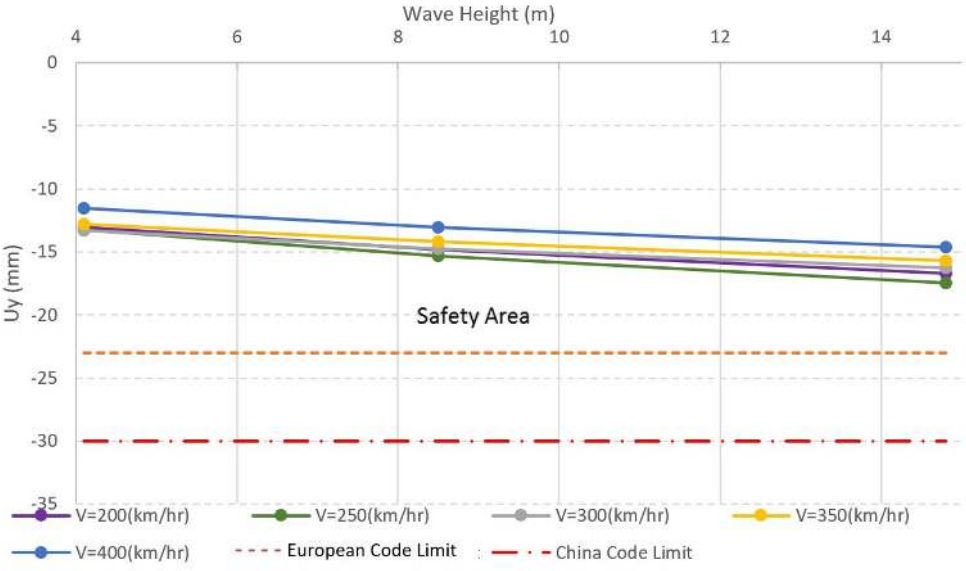


Figure 23- Response of Vertical Displacement under Train Speeds for Several Wave Height

By increasing height of the wave, lateral and vertical accelerations of deck increase and exceed the permissible values of the European and Chinese codes for most speeds except for V=200 km/h (as shown in figure 24 and 25). As shown in figure 24, it is possible for the train to pass at low speeds in stormy conditions, also it is possible for the train to pass at high speeds when sea-state is calm regarding to weather forecast. Lateral acceleration is more sensitive to speed when it increases from 200 km/h to 250 km/h. For other speeds trends are similar to 250 km/h. As shown in figure 25, when train speed increases, vertical acceleration is increased too. So it is possible to pass at high speeds when height of wave is low. Also it is possible to pass at low speeds in stormy conditions. Moreover it is possible for train to pass with speeds lower than 300 km/h in second sea-state. In this section, scenario 15 is considered as the maximum value.

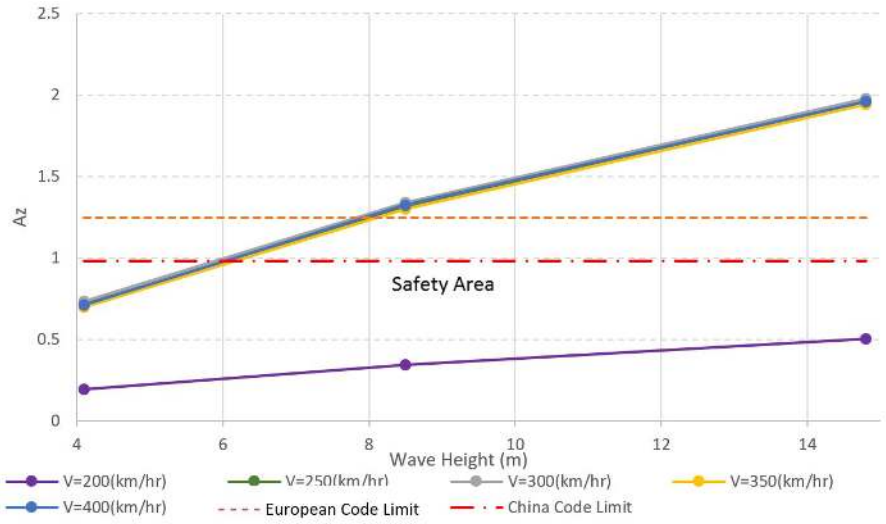


Figure 24- Response of Lateral Acceleration under Train Speeds for Several Wave Height

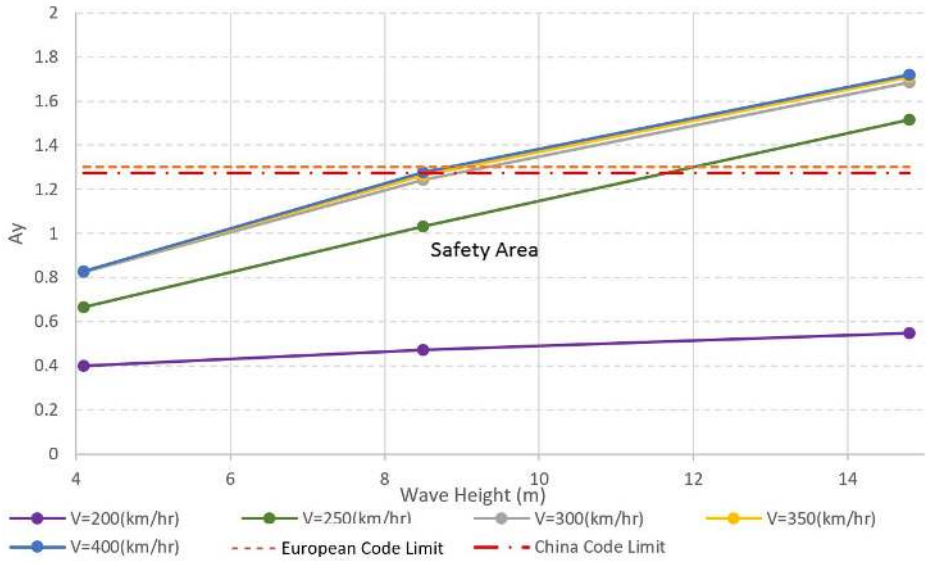


Figure 25- Response of vertical acceleration under train speeds for several wave height

6. CONCLUSION

The dynamic analysis of coupled train–bridge systems subjected to hydrodynamic loads is a rather complex problem, which is related to the running speed of the train, specification of car-body, train axle loads, specification of bridge, wave height, wave periods and length, the application position and the direction of the hydrodynamic load, and many other factors.

In this study, the dynamic behavior of the 3D train–bridge system subjected to different hydrodynamic loads (TBW model) is carried out. By taking a continuous bridge with (32 + 48 + 32) m box girders as a case study, the dynamic responses of the bridge in mid-span of bridge which is under train passing and subjected to several hydrodynamic loads are analyzed. An assessment procedure for the running safety of high-speed train on a bridge subjected to hydrodynamic load is proposed and related threshold curves for train speed versus several sea-states are defined.

The following conclusions can be drawn from sensitivity analyzes of TBW model under several train speeds and subjected to different sea-states:

(1) Hydrodynamic load has an obvious effect on the dynamic responses of the bridge. Both lateral and vertical displacements and accelerations responses of the bridge subjected to hydrodynamic load are much greater than the ones without hydrodynamic load.

(2) Vertical displacement and acceleration responses of the bridge subjected to stormy hydrodynamic load are 40% and 100% higher than the ones without hydrodynamic load, respectively.

(3) The lateral displacement and acceleration of the bridge are more influenced by hydrodynamic load. By applying hydrodynamic loads on piers and increasing the height of the wave, the lateral displacement and acceleration of the deck increase and exceed the permissible values of the European and Chinese codes.

(4) Lateral displacement response of the bridge subjected to stormy hydrodynamic load could be up to 26 times higher than the ones without hydrodynamic load.

(5) For vertical and lateral displacements, the most increase is observed between 200 km/h to 250 km/h and other speeds are distributed between them. Lateral displacement may not decrease considerable when train speed is decreased from 400 km/h to 250 km/h, and train speed shall be reduced under 250 km/h for safe and comfortable passing in harsh conditions.

(6) Vibrations induced by hydrodynamic load have a great effect on the dynamic responses of railway bridge and train running safety. The running safety of the train is affected by both the type of sea-state and train running speed. Strong waves may threaten the running safety of high-speed trains.

(7) Generally, the greater hydrodynamic load and the higher train speed, cause bigger influence on the running safety of the train. The running safety of the train could be evaluated by the threshold curve between train speed and hydrodynamic intensity.

(8) Results of TBW's sensitivity analyses have shown the importance of sea-states conditions for train safe and comfortable running.

(9) These outputs indicate that in stormy conditions such as sea state II or III ($H \geq 8.1$ m), the speed of the train crossing the bridges should be reduced and it is possible for the train to pass at low speeds such as 200 km/h in stormy conditions.

(10) In very stormy conditions like sea state III ($H = 14.8$ m), it is not safe for train running even at speed of 200 km/h.

Acknowledgment

We would also like to show our gratitude to Professor He Xia and Professor Nan Zhang from Beijing Jiao tong University for sharing their data for China High Speed Railway Bridge specifications with us during the course of this research, and we thank for their so-called insights.

Author's Contributions: Investigation and Writting, A Razzaghi Kalajahi; Methodologhy, A Razzaghi Kalajahi and M Esmaeili; Supervision, M Esmaeili and JA Zakeri

Editor: Pablo Andrés Muñoz Rojas.

References

Ataei, N., Stearns, M., Padgett, J. (2010). Response Sensitivity for Probabilistic Damage Assessment of Coastal Bridges under Surge and Wave Loading. Journal of the Transportation Research Board.

Bargi, K., Aghabozorgi, A. (2010). Dynamic Analysis of High Speed Train Passing on Bridge. Tehran University, Civil Department.

Bhaskar, A., Johnson, K.L., Wood, G.D., Woodhouse, G. (1997). Wheel-Rail Dynamics with Closely Conformal Contact, Part 1: Dynamic Modelling and Stability Analysis. Instn. Mech. Eng.

Bouassida, Y., Bouchon, E., Crespo, P., Croce, P., Davaine, L., Denton, S., Feldmann, M. (2012). Bridge Design to Eurocodes. JRC, European Commission. Vol. 1. https://doi.org/10.2788/82360.

Bradner, C., Schumacher, T., Asce, A., Cox, D., Higgins, C., Asce, M. (2011). Experimental Setup for a Large-Scale Bridge Superstructure Model Subjected to Waves. Journal of Waterway, Port, and Coastal Engineering 137 (1): 3–11. https://doi.org/10.1061/ASCEWW.1943-5460.0000059.

Cao, H. J., Yi, F., Feng, W. (2018). Estimate of the Extreme Wave Height in the South China Sea Using GPD Method. IOP Conference Series: Earth and Environmental Science 189 (5). https://doi.org/10.1088/1755-1315/189/5/052035.

CEN. (2005a). EN 1990-Eurocode - Basis of Structural Design.

CEN. (2005b). EN 1991- Eurocode: Actions on Structures.

CEN. (2005c). EN 1998- General Rules, Seismic Actions and Rules for Buildings.

Chakrabarti, SK. (1971). Discussion of Nondeterministic Analysis of Offshore Structures. Journal of the Engineering Mechanics.

Cuadrado, M., Gonzalez, P., Goicolea, J., Nasarre, J., Dias, R. (2008). Analysis of Lateral Displacements in Large Railway Viaducts under Traffic Loads. Impact on Ride Safety and Passenger Comfort. Proceedings of the 8th World Congress on Railway Research, 1–12.

Dadashzadeh, N., Zakeri, J. (2013). The Effect of Axial Load Changes on Railway Bridge's Response. International Congress on Civil Engineering, Architecture and Urban Sustainable Development in Iran.

De-gui, B., Guo-xing, C., Zhi-hua, W. (2008). Seismic Response Analysis of the Large Bridge Pier Supported By Group Pile Foundation Considering the Effect of Wave and Current Action.

Dias, R., Silva, F. (2007). Dynamic Behaviour of High Speed Railway Bridges. Vehicles Lateral Dynamic Behaviour. Civil Engineering, no. November: 172.

Eicher, J. A., Guan, H., Jeng, D. (2003). Stress and Deformation of Offshore Piles under Structural and Wave Loading. Ocean Engineering 30 (3): 369–85. https://doi.org/10.1016/S0029-8018(02)00031-8.

Ellis, B. R., Ji, T., Bell, J. (2003). Horizontal Movements of Frame Structures Induced by Vertical Loads. Proceedings of the ICE - Structures and Buildings 156 (2): 141–50. https://doi.org/10.1680/stbu.2003.156.2.141.

Fang, C., Yongle, L., Kai, W., Jingyu, Z., Chunming, L. (2018). Vehicle – Bridge Coupling Dynamic Response of Sea-Crossing Railway Bridge under Correlated Wind and Wave Conditions. Advances in Structural Engineering. https://doi.org/10.1177/1369433218781423.

Frýba, L. (1996). Dynamics of Railway Bridges. Thomas Telford Publishing.

Hassan, A., Saddiq, E. (2016). TRANSIENT STRESS ANALYSIS OF SIMPLY SUPPORT BEAM EXCITED UNDER MOVING LOAD. Al-Qadisiyah Journal For Engineering Sciences 9 (3): 331–48.

Höghastighetsprojekt, B. (2010). Delrapport 1, KTH Kungliga Tekniska Högskolan, TRITA-BKN Rapport 139.

Hughes, S. (2010). A Critical Analyis of the Øresund Bridge, Connecting Copenhagen To Malmö. Transportation Research Record Journal of the Transportation Research Board 1654(1):133-140.

Indian Institute of Technology. (2010). IITK-RDSO GUIDELINES ON SEISMIC DESIGN OF RAILWAY BRIDGES.

ISO. (2002). ISO 2631- Mechanical Vibration and Shock- Evaluation of Human Exposure to Whole-Body Vibration.

Jahangiri, M., Zakeri, Z. (2017). Dynamic Analysis of Train-Bridge System under One-Way and Two-Way High-Speed Train Passing. Structural Engineering and Mechanics 64 (1): 33–44. https://doi.org/10.12989/sem.2017.64.1.033.

James, G. (2003). Analysis of traffic load effects an railway bridges (Doctoral dissertation, Byggvetenskap).

Jeon, B., Nam Sik, K., Sung Il, K. (2016). Estimation of the Vibration Serviceability Deflection Limit of a High-Speed Railway Bridge Considering the Bridge-Train Interaction and Travel Speed. KSCE Journal of Civil Engineering 20 (2): 747–61. https://doi.org/10.1007/s12205-015-0565-z.

Ji, J., Wenfu, Z., Wenyan, Z., Chaoqing, Y., Yang, Y. (2012). Analysis and Comparison on Dynamic Characteristics of the Bridge Subjected to Moving Load Based on ANSYS. Journal of Convergence Information Technology 7 (8): 159–68. https://doi.org/10.4156/jcit.vol7.issue8.18.

Jiang, Y., Bernard, K., Cameron, T. (2019). A Comparison Study of Ride Comfort Indices between Sperling's Method and EN 12299. International Journal of Rail Transportation 7 (4): 279–96. https://doi.org/10.1080/23248378.2019.1616329.

K.Liu., De Roeck, G., Lombaert, G. (2009). The Effect of Dynamic Train-Bridge Interaction on the Bridge Response during a Train Passage. Journal of Sound and Vibration.

Kaloop, M., Jong, Hu., Emad, E. (2016). Evaluation of High-Speed Railway Bridges Based on a Nondestructive Monitoring System. Applied Sciences 6 (1): 24. https://doi.org/10.3390/app6010024.

Karadeniz, H. (1999). Spectral Analysis of Offshore Structures under Combined Wave and Earthquake Loadings. Proceedings of the 1999 Ninth International Offshore and Polar Engineering Conference (Volume 4), Brest, France, 30 May - 4 June 1999 IV: 504–11. http://www.scopus.com/inward/record.url?eid=2-s2.0-0033508612&partnerID=tZOtx3y1.

Kitada, T. (2006). Considerations on Recent Trends in, and Future Prospects of, Steel Bridge Construction in Japan. Journal of Constructional Steel Research.

Li, F., Guoxing, C., Zhihua, W. (2008). Seismic Responses of Bridge Pier Considering the Effect of Hydrodynamic Pressure. Science Press Beijing and Springer-Verlag GmbH Berlin Heidelberg Geotechnical Engineering for Disaster Mitigation and Rehabilitation, no. 1977.

Li, Y., Jiangtao, D., Bin, W., Chuanjin, Yu. (2015). Running Safety of Trains under Vessel-Bridge Collision. Shock and Vibration 2015. https://doi.org/10.1155/2015/252574.

Melaku, S., Hongsheng, Q. (2014). Transient Dynamic Analysis of Simple Railway Bridge under Train Moving Load. International Conference on Civil Engineering, Energy and Environment.

Ministry of Railways of the People's Republic of China. (2009). Code for Design of High-Speed Railway (China).

Miyata, T., Koji, Y. (1993). Aerodynamics of Wind Effects on the Akashi Kaikyo Bridge. Journal of Wind Engineering and Industrial Aerodynamics 48 (2–3): 287–315. https://doi.org/10.1016/0167-6105(93)90142-B.

Museros, P., Romero, M., Poy, A., Alarcon, E. (2002). Advances in the Analysis of Short Span Railway Bridges for High-Speed Lines. Computers & Structures.

Rashid, Sh. (2011). Parametric Study of Bridge Response to High Speed Trains. Ballasted Track on Concrete Bridges.

Rigueiro, C., Rebelo, C., Simoes da Silva, L. (2010). Influence of Ballast Models in the Dynamic Response of Railway Viaducts. Journal of Sound and Vibration.

Robertson, I., Riggs, H., Yim, S. (2007). Lessons from Hurricane Katrina Storm Surge on Bridges and Buildings. Journal of Waterway, Port, Coastal, and Ocean Engineering.

Song, B. (2010). Study on the Calculation Method for Hydrodynamic Pressure of Bridge Piers in Deep Water under Earthquakes. University of Science and Technology Beijing Main Contents.

Sorensen, R. (1993). Basic Wave Mechanics for Ocean Engineering. New York: John Wiley.

Unsworth, J. (2010). Design of Modern Steel Railway Bridges. Structure and Infrastructure Engineering.

Varandas, J., Paul, H., Manuel, S. (2011). Dynamic Behaviour of Railway Tracks on Transition Zones. Computers & Structures.

Wang, Z., Chong, S., Guo, X. (2011). Seismic Response of Bridge Pier in Deep Water Considering Close Fluid-Structure Interaction Effects. Advanced Materials Research 243–249: 1803–10. https://doi.org/10.4028/www.scientific.net/AMR.243-249.1803.

Watanabe, E., Tomoaki, U. (2003). Analysis and Design of Floating Bridges. Progress in Structural Engineering and Materials 5 (3): 127–44. https://doi.org/10.1002/pse.151.

Xia, C. Y., Lei, J., Zhang, N., Xia, H., De Roeck, G. (2012). Dynamic Analysis of a Coupled High-Speed Train and Bridge System Subjected to Collision Load. Journal of Sound and Vibration 331 (10): 2334–47. https://doi.org/10.1016/j.jsv.2011.12.024.

Xia, C. Y., Xia, H., De Roeck, G. (2014). Dynamic Response of a Train-Bridge System under Collision Loads and Running Safety Evaluation of High-Speed Trains. Computers and Structures 140: 23–38. https://doi.org/10.1016/j.compstruc.2014.04.010.

Xia, C, Jin, M., Xia, H. (2015). Dynamic Analysis of a Train-Bridge System to Vessel Collision and Running Safety of High-Speed Trains. Vibroengineering PROCEDIA, Vol. 5, p. 509-514.

Xia, H., Zhang, N. (2005). Dynamic Analysis of Railway Bridge under High-Speed Trains. Computers and Structures 83 (23–24): 1891–1901. https://doi.org/10.1016/j.compstruc.2005.02.014.

Yasuda, M., Kitagawa, M., Moritni, T., Fukunaga, S. (2000). Seismic Design and Behavior During the Hyogo-Ken Nanbu Earthquake of the Akashi Kaikyo Bridge. Proc. 12th World Conference on Earthquake Engineering, Auckland, New Zealand Paper No.: 3–10.

Yim, S. (2005). Modeling and Simulation of Tsunami and Storm Surge Hydrodynamic Loads on Coastal Bridge Structures. 21st US Japan Bridge Engineering Workshop, no. April: 1–14.

Yim, W. T. (2007). Akashi Bridge. In Proceedings of Bridge Engineering 2end Conference, Japan.